Hindawi
Advances in Mathematical Physics
Volume 2023, Article ID 9996101, 14 pages
https://doi.org/10.1155/2023/9996101

Research Article

Fractional Soliton and Semirational Solutions of a Fractional Two-Component Generalized Hirota Equation

Sheng Zhang,[1] **Feng Zhu**,[1] **and Bo Xu**[2]

[1]*School of Mathematical Sciences, Bohai University, Jinzhou 121013, China*
[2]*School of Educational Sciences, Bohai University, Jinzhou 121013, China*

Correspondence should be addressed to Sheng Zhang; szhangchina@126.com

Received 25 May 2023; Revised 13 September 2023; Accepted 16 September 2023; Published 16 October 2023

Academic Editor: Carlo Bianca

Copyright © 2023 Sheng Zhang et al. This is an open access article distributed under the Creative Commons Attribution License, which permits unrestricted use, distribution, and reproduction in any medium, provided the original work is properly cited.

The Darboux transformation (DT) and generalized DT (GDT) have played important roles in constructing multisoliton solutions, rogue wave solutions, and semirational solutions of integrable systems. The main purpose of this article is to extend the DT and GDT to a conformable fractional two-component generalized Hirota (TCGH) equation for revealing novel dynamic characteristics of fractional soliton and semirational solutions. As for the main contributions, specifically, we propose a fractional form of the TCGH equation, provide the associated fractional Lax pair, and obtain fractional soliton and semirational solutions of the fractional TCGH equation by constructing its fractional DT and GDT. In addition, we find that the dominant role of fractional order leads to new dynamic characteristics of the obtained fractional soliton and semirational solutions, mainly including a certain degree of tilt of wave crests and the variations in velocities and wave widths over time during propagation, which are not possessed by the corresponding integer-order TCGH equation. Meanwhile, this study predicts the deceleration propagation of solitons in fractional dimensional media and brings the possibility of exploring the asymmetric regulation mechanism of rogue waves from the perspective of fractional-order dominance.

1. Introduction

Fractional calculus is very important and has a wide range of applications [1]. As pointed out in [2], a connection between fractional calculus and soliton theory can be established. This makes it meaningful to generalize soliton integrable systems to fractional orders, such as the fractional-order version [3] of classical nonlinear Schrödinger (NLS) equation. Recently, more and more fractional nonlinear integrable systems have been proposed, such as the fractional Korteweg–de Vries (KdV) equation [4], fractional isospectral and nonisospectral Ablowitz–Kaup–Newell–Segur (AKNS) hierarchies [5], fractional Kadomtsev–Petviashvili (KP) equation [6], fractional NLS equation [7], fractional modified KdV (mKdV) equation [8], fractional discrete NLS equation [9], fractional NLS hierarchy [10], and higher-order fractional NLS equation [11]. As is well known, studying ocean waves is of great significance for human development. Researchers often use some soliton integrable equations, for example, the KP equation [12], to study water wave motion. Wave motion is one of the most common phenomena in the ocean and has its importance for coastal engineering, harbor construction, and the evolution of beaches. The KP equation [12], can be seen as an extension of the famous KdV equation [13] to two-dimensional space, is an important model for simulating ocean waves. One of the higher-order NLS equations, known as the celebrated Hirota equation [14], is a combination of the NLS equation and the complex mKdV equation.

Due to the importance [14–19] of studying the Hirota equation and its generalizations, this paper considers the following fractional two-component generalized Hirota (TCGH) equation:

$$\begin{aligned} &iD_t^\alpha u + \frac{1}{2}D_x^{2\alpha}u + (|u|^2 + |v|^2)u + \frac{i}{12}(D_x^{3\alpha}u + (6|u|^2 + 3|v|^2)D_x^\alpha u + 3uv^* D_x^\alpha v) = 0 \\ &iD_t^\alpha v + \frac{1}{2}D_x^{2\alpha}v + (|u|^2 + |v|^2)v + \frac{i}{12}(D_x^{3\alpha}v + (6|v|^2 + 3|u|^2)D_x^\alpha v + 3vu^* D_x^\alpha u) = 0 \end{aligned}, \ (0<\alpha\le 1), \tag{1}$$

where $|u|$ and $|v|$ are two modules of the slowly varying complex envelop potentials $u(x,t)$ and $v(x,t)$, $i^2 = -1$ gives the imaginary unit, * represents the complex conjugation, while D_t^α, D_x^α, $D_x^{2\alpha} = D_x^\alpha D_x^\alpha$ and $D_x^{3\alpha} = D_x^\alpha D_x^\alpha D_x^\alpha$ denote the conformable fractional derivatives with respect to t and x [6, 20]. When $\alpha = 1$, Equation (1) degenerates into the integer-order TCGH equation [21] with the strength parameter $\varepsilon = 1/12$ identifying the high-order effects from the third dispersion, self-steepening, and the so-called inelastic Raman scattering [15]. In the fields of optics and ocean dynamics, the integer-order case of Equation (1) can be used to illustrate the transmission process of high-intensity ultrashort pulses through an optical glass fiber [17] and deep water ocean wave collisions caused by the adverse weather conditions [18].

As far as we know, the fractional TCGH Equation (1) is new, and its fractional soliton solutions and semirational solutions have not been reported. From a mathematical point of view, semirational solutions are a kind of rational exact solutions coupled by e-exponential functions and external independent variables. In terms of the spatial structures, semirational solutions usually exhibit local characteristics of solitons and rogue waves. There are many effective methods for constructing exact solutions of nonlinear evolution systems, for example, the inverse scattering transform [22], Hirota bilinear method [23], homogeneous balance method [24], and exp-function method [25]. Because this paper focuses on solving fractional integrable systems, we also introduce some methods such as Adomian decomposition method [26], variational iteration method [27], and homotopy perturbation method [28] used in recent literature to handle fractional-order nonlinear equations. Traditional Darboux transformation (DT) [29] can construct the well-known soliton solutions, while the generalized DT (GDT) [30] based on DT [29] was originally designed to obtain rational solutions and has recently been applied to the construction of rogue wave solutions [31] and semirational solutions [32]. In this present paper, we concentrate on constructing novel fractional soliton and semirational solutions of the fractional TCGH Equation (1) by introducing fractional DT and GDT. The fractional DT and GDT mentioned in this paper emphasize that the Lax pair they are based on is in the form of fractional derivatives, and the series of operations processed involve spatiotemporal variables that are all fractional powers. These aspects are different from those of the traditional DT [29] and GDT [30]. Although we have some preliminary studies [33, 34] on fractional DT and GDT, the starting point of this work is to reveal the novel dynamic characteristics dominated by fractional order of fractional soliton and semirational solutions from a new fractional integrable system.

For the fractional TCGH Equation (1), considering the needs of the next section, here we give its fractional Lax pair:

$$D_x^\alpha \varphi = M\varphi, M = \lambda U_0 + U_1, \tag{2}$$

$$D_t^\alpha \varphi = N\varphi, N = \lambda^3 V_0 + \lambda^2 V_1 + \lambda V_2 + V_3, \tag{3}$$

in which φ represents the eigenfunction, λ is the eigenvalue, and

$$\begin{aligned} &U_0 = \begin{bmatrix} -2i & 0 & 0 \\ 0 & i & 0 \\ 0 & 0 & i \end{bmatrix}, \ U_1 = \begin{bmatrix} 0 & -u & -v \\ u^* & 0 & 0 \\ v^* & 0 & 0 \end{bmatrix}, \\ &V_0 = \frac{3}{4}U_0, V_1 = \frac{3}{2}U_0 + \frac{3}{4}U_1, \end{aligned} \tag{4}$$

$$V_2 = \frac{1}{4}\begin{bmatrix} ie_0 & -6u - iD_x^\alpha u & -6v - iD_x^\alpha v \\ 6u^* - iD_x^\alpha u^* & -i|u|^2 & -ivu^* \\ 6v^* - iD_x^\alpha v^* & -iuv^* & -i|v|^2 \end{bmatrix}, \tag{5}$$

$$V_3 = \begin{bmatrix} \frac{1}{12}(e_1 + e_2) + \frac{i}{2}e_0 & \frac{1}{12}e_3 - \frac{i}{2}u_x & \frac{1}{12}e_4 - \frac{i}{2}v_x \\ -\frac{1}{12}e_3^* - \frac{i}{2}u_x^* & -\frac{1}{12}e_1 - \frac{i}{2}|u|^2 & \frac{1}{12}e_5 - \frac{i}{2}vu^* \\ -\frac{1}{12}e_4^* - \frac{i}{2}v_x^* & -\frac{1}{12}e_5^* - \frac{i}{2}uv^* & -\frac{1}{12}e_2 - \frac{i}{2}|v|^2 \end{bmatrix}, \tag{6}$$

with

$$e_0 = |u|^2 + |v|^2, e_1 = uD_x^\alpha u^* - u^* D_x^\alpha u, e_2 = vD_x^\alpha v^* - v^* D_x^\alpha v, \tag{7}$$

$$e_3 = D_x^{2\alpha}u + 2e_0 u, e_4 = D_x^{2\alpha}v + 2e_0 v, e_5 = u^* D_x^\alpha v - vD_x^\alpha u^*. \tag{8}$$

The framework of this paper is organized as follows. In Section 2, we derive the fractional DT and GDT of Equation (1) by extending the DT [29] and GDT [30]. Based on the derived GDT, fractional soliton and semirational solutions of Equation (1) are obtained in Section 3. At the same time, dynamic features of the obtained fractional soliton and semirational solutions are analyzed. The last section is the summary and discussion of this paper.

2. Fractional DT and GDT

In this section, following the steps of the DT [29] and GDT [30], we present the fractional DT and GDT for the fractional TCGH Equation (1).

2.1. Fractional DT. To give the fractional DT for the fractional TCGH Equation (1), we begin with a special gauge transformation:

$$\varphi^{[1]} = T\varphi = (\lambda I_3 - S)\varphi = (\lambda I_3 - H\Lambda H^{-1})\varphi\,, \tag{9}$$

with

$$\Lambda = \begin{bmatrix} \lambda_1 & 0 & 0 \\ 0 & \lambda_1^* & 0 \\ 0 & 0 & \lambda_1^* \end{bmatrix}, H = \begin{bmatrix} \varphi_{11} & \varphi_{12}^* & \varphi_{13}^* \\ \varphi_{12} & -\varphi_{11}^* & 0 \\ \varphi_{13} & 0 & -\varphi_{11}^* \end{bmatrix}, \tag{10}$$

where $(\varphi_{11}, \varphi_{12}, \varphi_{13})^T$ is a solution of the fractional Lax pair, as shown in Equations (2) and (3), in the case of $\lambda = \lambda_1$, and $(\varphi_{12}^*, -\varphi_{11}^*, 0)^T$and $(\varphi_{13}^*, 0, -\varphi_{11}^*)^T$ satisfy the fractional Lax pair, as shown in Equations (2) and (3), when $\lambda = \lambda_1^*$.

According to the rules of fractional DT: $D_x^\alpha T + TM = M^{[1]}T, D_t^\alpha T + TN = N^{[1]}T$, we obtain the following relations between former and new potentials by comparing the coefficients of the same powers of λ:

$$U_1^{[1]}S = D_x^\alpha S + SU_1\,, \tag{11}$$

$$V_3^{[1]}S = D_x^\alpha S + SV_3\,, \tag{12}$$

$$U_1^{[1]} = U_1 - SU_0 + U_0 S\,, \tag{13}$$

$$V_3^{[1]} - V_2^{[1]}S = V_3 - SV_2\,, \tag{14}$$

$$V_2^{[1]} - \frac{3}{4}U_1^{[1]}S = V_2 - \frac{3}{2}SU_0 - \frac{3}{4}SU_1 + \frac{3}{2}U_0 S\,. \tag{15}$$

Through direct computation, we arrive at the potential formulas:

$$u^{[1]} = u + 3i(\lambda_1 - \lambda_1^*)\frac{\varphi_{11}\varphi_{12}^*}{|\varphi_{11}|^2 + |\varphi_{12}|^2 + |\varphi_{13}|^2}\,, \tag{16}$$

$$v^{[1]} = v + 3i(\lambda_1 - \lambda_1^*)\frac{\varphi_{11}\varphi_{13}^*}{|\varphi_{11}|^2 + |\varphi_{12}|^2 + |\varphi_{13}|^2}\,. \tag{17}$$

By means of the above preparations, the first step of fractional DT of the fractional TCGH Equation (1) can be written in a more straightforward way, that is:

$$T_1 = (\lambda - \lambda_1^*)I_3 - (\lambda_1 - \lambda_1^*)\frac{\varphi_1\varphi_1^H}{\varphi_1^H\varphi_1}\,, \tag{18}$$

$$u^{[1]} = u + 3i(\lambda_1 - \lambda_1^*)\left(\frac{\varphi_1\varphi_1^H}{\varphi_1^H\varphi_1}\right)_{12}\,, \tag{19}$$

$$v^{[1]} = v + 3i(\lambda_1 - \lambda_1^*)\left(\frac{\varphi_1\varphi_1^H}{\varphi_1^H\varphi_1}\right)_{13}\,, \tag{20}$$

where the column vector $\varphi_1 = (\varphi_{11}, \varphi_{12}, \varphi_{13})^T$ solves the fractional Lax pair, as shown in Equations (2) and (3), with $\lambda = \lambda_1$, and H denotes the transpose and complex conjugation of the vector being acted on.

As shown in Equations (18)–(20), the fractional DT of degree one has been presented. The N-fold fractional DT for the fractional TCGH Equation (1) can be considered as a superposition of the first-step fractional DT, namely:

$$T_n = (\lambda - \lambda_n^*)I_3 - (\lambda_n - \lambda_n^*)\frac{\varphi_n\varphi_n^H}{\varphi_n^H\varphi_n}\,, \tag{21}$$

$$u^{[n]} = u + 3i\sum_{m=1}^{n}(\lambda_m - \lambda_m^*)\left(\frac{\varphi_m\varphi_m^H}{\varphi_m^H\varphi_m}\right)_{12}\,, \tag{22}$$

$$v^{[n]} = v + 3i\sum_{m=1}^{n}(\lambda_m - \lambda_m^*)\left(\frac{\varphi_m\varphi_m^H}{\varphi_m^H\varphi_m}\right)_{13}\,, \tag{23}$$

where $\varphi_m = (\varphi_{m1}, \varphi_{m2}, \varphi_{m3})^T$ satisfies the fractional Lax pair, as shown in Equations (2) and (3), given by $\lambda = \lambda_m$.

2.2. Fractional GDT. With the help of above fractional DT, we get $T_1\varphi_1 = 0$. In this case, we cannot try to apply the fractional DT on φ_1 again. Setting $\gamma^{[1]} = \varphi_1(\lambda_1 + \delta)$ and expanding $\gamma^{[1]}$ at λ_1, we find that:

$$\gamma^{[1]} = \varphi_1(\lambda_1 + \delta) = {\gamma_0}^{[1]} + {\gamma_1}^{[1]}\delta + {\gamma_2}^{[1]}\delta^2 + \cdots + {\gamma_n}^{[1]}\delta^n + \cdots\,, \tag{24}$$

where

$$\gamma_k^{[1]} = \frac{1}{k!}\frac{\partial^k}{\partial\lambda^k}\varphi_1(\lambda)\big|_{\lambda=\lambda_1},\quad (k = 0, 1, 2, \cdots). \tag{25}$$

As ${\gamma_0}^{[1]} = \varphi_1(\lambda_1)$ satisfies the fractional Lax pair, as shown in Equations (2) and (3), with the given $\lambda = \lambda_1$ and seed solutions u and v, we can drive the first-step fractional GDT of the fractional TCGH Equation (1):

$$T_1[1] = (\lambda - \lambda_1^*)I_3 - (\lambda_1 - \lambda_1^*)\frac{\varphi_1\varphi_1^H}{\varphi_1^H\varphi_1}\,, \tag{26}$$

$$u[1] = u + 3i(\lambda_1 - \lambda_1^*)\left(\frac{\varphi_1\varphi_1^H}{\varphi_1^H\varphi_1}\right)_{12}\,, \tag{27}$$

$$v[1] = v + 3i(\lambda_1 - \lambda_1^*)\left(\frac{\varphi_1\varphi_1^H}{\varphi_1^H\varphi_1}\right)_{13}\,. \tag{28}$$

Since φ_1 has been determined in Equations (18)–(20), then comparing Equations (26)–(28) with Equations (18)

and (19), we conclude that there is no difference between the fractional DT and fractional GDT in the first iteration.

In what follows, we derive the second-step fractional GDT of the fractional TCGH Equation (1) through the limit process:

$$\lim_{\delta\to 0}\frac{\left[T_1[1]\big|_{\lambda=\lambda_1+\delta}\right]\gamma^{[1]}}{\delta}=\lim_{\delta\to 0}\frac{\left[\delta+T_1[1]\big|_{\lambda=\lambda_1}\right]\gamma^{[1]}}{\delta}=\gamma_0^{[1]}+T_1[1]\big|_{\lambda=\lambda_1}\gamma_1^{[1]}=\varphi_1[1]\,, \tag{29}$$

where $\gamma_0^{[1]}$ and $\gamma_1^{[1]}$ have been determined in Equation (24). Thus, $\varphi_1[1]$ which is the next iterative function after φ_1 can be determined by means of Equation (29). When $n=2$, Equation (21) can be written as:

$$T_2=(\lambda-\lambda_2^*)I_3-(\lambda_2-\lambda_2^*)\frac{\varphi_2\varphi_2^H}{\varphi_2^H\varphi_2}\,. \tag{30}$$

Taking the limit $\lambda_2\to\lambda_1$ and substituting the new iterated eigenfunction $\varphi_1[1]$ into Equation (30), we can derive the second-step fractional GDT of the fractional TCGH Equation (1), that is:

$$T_1[2]=(\lambda-\lambda_1^*)I_3-(\lambda_1-\lambda_1^*)\frac{\varphi_1[1]\varphi_1^H[1]}{\varphi_1^H[1]\varphi_1[1]}\,, \tag{31}$$

$$u[2]=u[1]+3i(\lambda_1-\lambda_1^*)\left(\frac{\varphi_1[1]\varphi_1^H[1]}{\varphi_1^H[1]\varphi_1[1]}\right)_{12}, \tag{32}$$

$$v[2]=v[1]+3i(\lambda_1-\lambda_1^*)\left(\frac{\varphi_1[1]\varphi_1^H[1]}{\varphi_1^H[1]\varphi_1[1]}\right)_{13}. \tag{33}$$

Similarly, we acquire the third iterated eigenfunction $\varphi_1[2]$ via the following limit process:

$$\lim_{\delta\to 0}\frac{[T_1[2](\lambda_1+\delta)]\left[\frac{\delta+T_1[1](\lambda_1)}{\delta}\right]\gamma^{[1]}}{\delta}\,, \tag{34}$$

$$=\gamma_0^{[1]}+[T_1[1](\lambda_1)+T_1[2](\lambda_1)]\gamma_1^{[1]}+T_1[2](\lambda_1)T_1[1](\lambda_1)\gamma_2^{[1]}=\varphi_1[2]\,, \tag{35}$$

where $\gamma_0^{[1]},\gamma_1^{[1]}$and $\gamma_2^{[1]}$ are already determined, as shown in Equation (25). Then, the third-step fractional GDT is derived as follows:

$$T_1[3]=(\lambda-\lambda_1^*)I_3-(\lambda_1-\lambda_1^*)\frac{\varphi_1[2]\varphi_1^H[2]}{\varphi_1^H[2]\varphi_1[2]}\,, \tag{36}$$

$$u[3]=u[2]+3i(\lambda_1-\lambda_1^*)\left(\frac{\varphi_1[2]\varphi_1^H[2]}{\varphi_1^H[2]\varphi_1[2]}\right)_{12}, \tag{37}$$

$$v[3]=v[2]+3i(\lambda_1-\lambda_1^*)\left(\frac{\varphi_1[2]\varphi_1^H[2]}{\varphi_1^H[2]\varphi_1[2]}\right)_{13}. \tag{38}$$

3. Fractional Soliton and Semirational Solutions

In this section, we employ the fractional GDT derived above to construct fractional semirational solutions of the fractional TCGH Equation (1).

3.1. Fractional Soliton Solutions. Starting from the seed solutions $u=0$ and $v=0$, we solve the fractional Lax pair, as shown in Equations (2) and (3), with $\lambda=\lambda_1$ and yield that:

$$\varphi_1=\begin{bmatrix}c_1e^{-2i\theta}\\ c_2e^{i\theta}\\ c_3e^{i\theta}\end{bmatrix},\ \theta=\frac{\lambda_1}{\alpha}x^\alpha+\frac{3\lambda_1^2(\lambda_1+2)}{4\alpha}t^\alpha\,, \tag{39}$$

where c_1, c_2 and c_3 are complex constants. Substituting Equation (39) into Equations (27) and (28), we can derive the fractional one-soliton solutions of the fractional TCGH Equation (1):

$$u[1]=\frac{3i(\lambda_1-\lambda_1^*)c_1c_2^*}{|c_1|^2e^{3i\theta^*}+|c_2|^2e^{3i\theta}+|c_3|^2e^{3i\theta}}\,, \tag{40}$$

$$v[1]=\frac{3i(\lambda_1-\lambda_1^*)c_1c_3^*}{|c_1|^2e^{3i\theta^*}+|c_2|^2e^{3i\theta}+|c_3|^2e^{3i\theta}}\,. \tag{41}$$

Especially when $\lambda_1=i$, $c_1=1$, $c_2=1$, and $c_3=1$, we simplify Equations (40) and (42) as follows:

$$u[1]=v[1]=-\frac{6e^{\frac{9(1+2i)}{4\alpha}t^\alpha+\frac{3}{\alpha}x^\alpha}}{2e^{\frac{9}{2\alpha}t^\alpha}+e^{\frac{6}{\alpha}x^\alpha}}=-\frac{3\sqrt{2}}{2}e^{\frac{9i}{2\alpha}t^\alpha}\operatorname{sech}\left(\frac{3}{\alpha}x^\alpha-\frac{9}{4\alpha}t^\alpha-\ln\sqrt{2}\right). \tag{42}$$

As shown in Figures 1–3, four right propagating single solitons with different fractional orders $\alpha=1,\alpha=7/9,\alpha=3/5$, and $\alpha=1/3$ are shown. As shown in Figures 1–3, when t is fixed to three different moments -1, 0, and 1, the smaller the value of fractional order α, the narrower the wave width, and the greater the tilt of wave crest toward the vertical axis. But soon, as shown in Figure 4, with the gradual disappearance of the tilt, the wave peaks become wider and wider, until the change becomes very slow or no longer occurs after a long time. When $t=3{,}000$, the wave peak with the fractional order $\alpha=1/3$, as shown in Figure 5, has almost no tilt.

As for the velocity of the fractional single soliton determined by Equation (42), we have the following formulae:

$$v=3^{\frac{2\alpha-1}{\alpha}}4^{-\frac{1}{\alpha}}t^{\alpha-1}(9t^\alpha+2\alpha\ln 2)^{\frac{1-\alpha}{\alpha}},\ \alpha\in(0,1)\,, \tag{43}$$

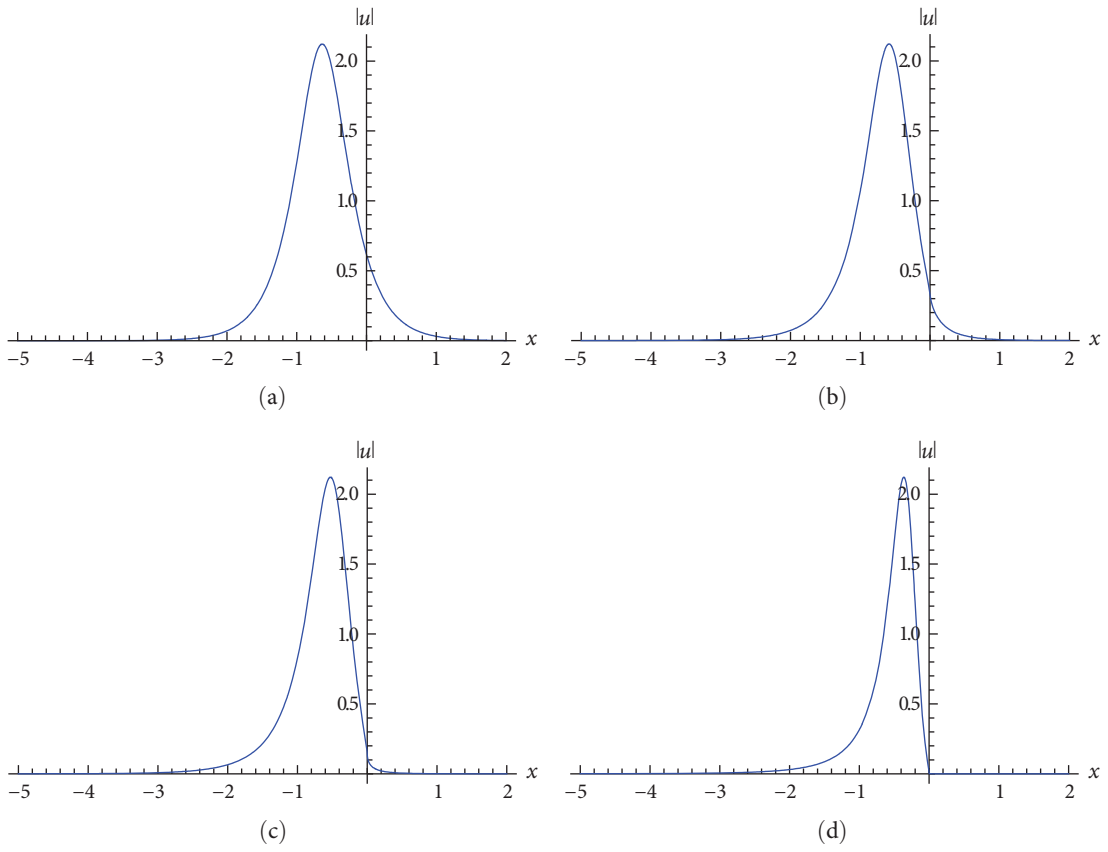

Figure 1: Fractional single solitons determined by Equation (42) with the different fractional orders: (a) $\alpha = 1$, (b) $\alpha = 7/9$, (c) $\alpha = 3/5$, and (d) $\alpha = 1/3$ at the time $t = -1$.

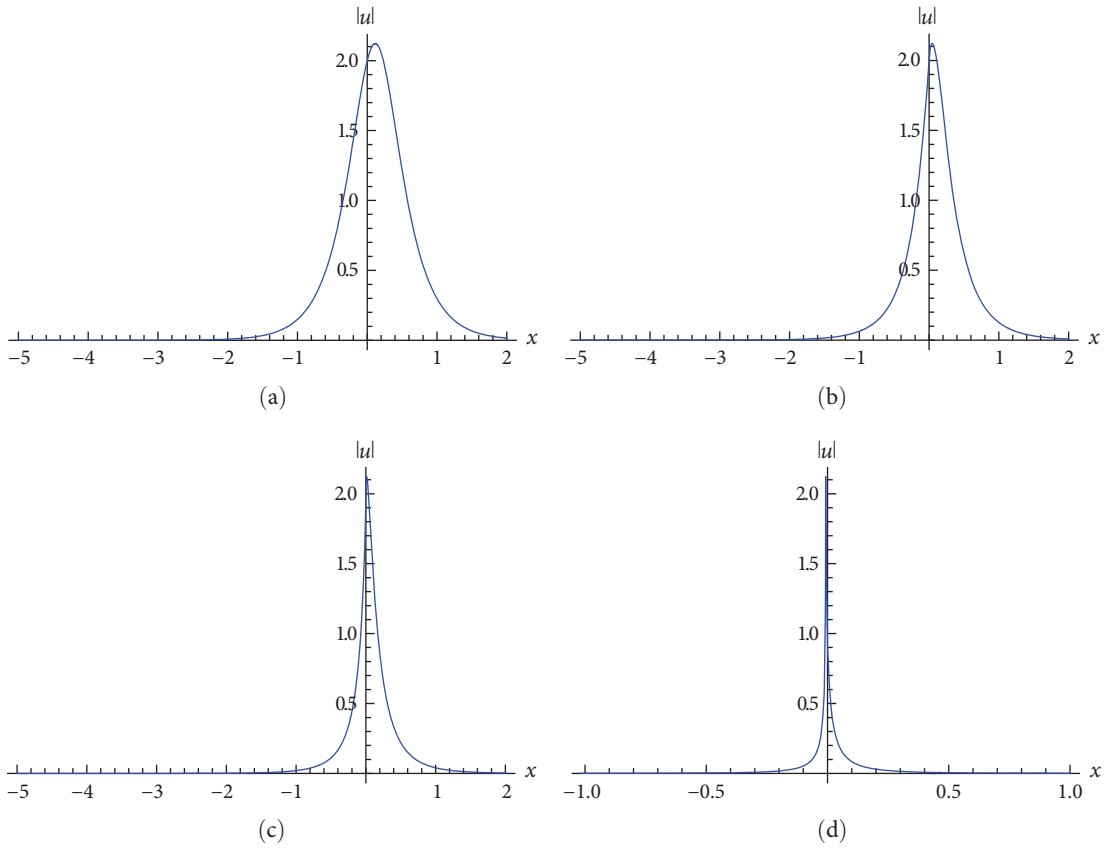

Figure 2: Fractional single solitons determined by Equation (42) with the different fractional orders: (a) $\alpha = 1$, (b) $\alpha = 7/9$, (c) $\alpha = 3/5$, and (d) $\alpha = 1/3$ at the time $t = 0$.

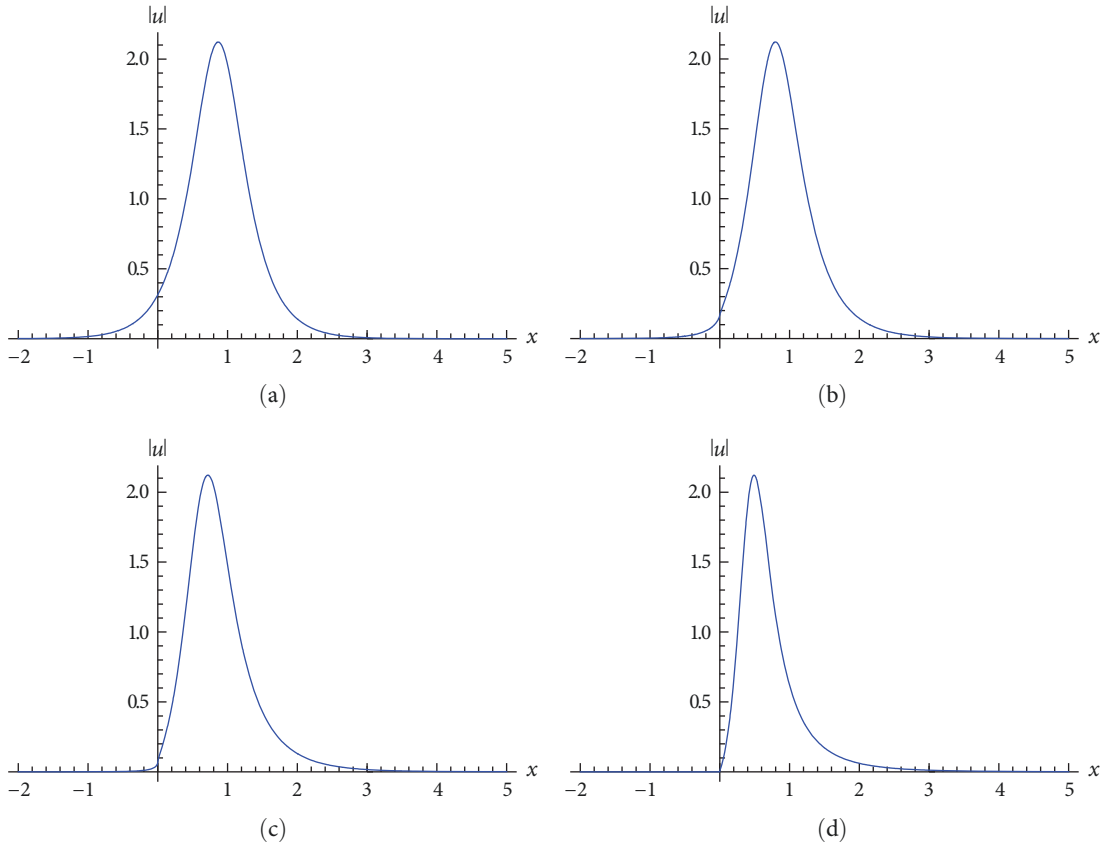

Figure 3: Fractional single solitons determined by Equation (42) with the different fractional orders: (a) $\alpha = 1$, (b) $\alpha = 7/9$, (c) $\alpha = 3/5$, and (d) $\alpha = 1/3$ at the time $t = 1$.

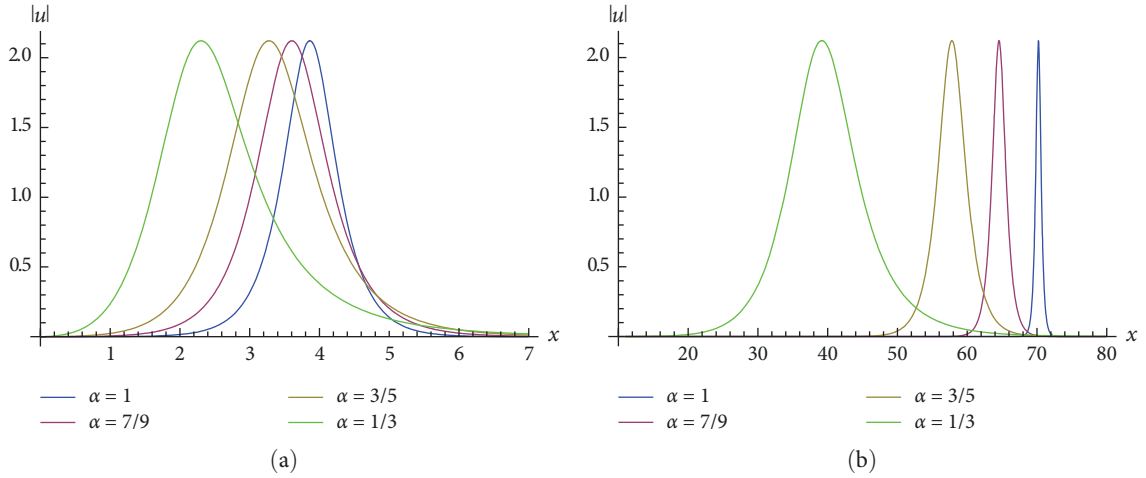

Figure 4: Fractional single solitons determined by Equation (42) with the different fractional orders $\alpha = 1$, $\alpha = 7/9$, $\alpha = 3/5$, and $\alpha = 1/3$ at the times: (a) $t = 5$ and (b) $t = 100$.

$$v = \frac{3}{4}, \ (\alpha = 1), \tag{44}$$

which tell that in the case of $\alpha = 1$, the velocity, as shown in Equation (44), is the constant $3/4$, while for $0 < \alpha < 1$, it is time-varying. When confining the fractional order $\alpha \in (0, 1)$ and time interval $t \in [0.001, 1{,}000]$, we show the 3D image of velocity, as shown in Equation (43) (Figure 6). Four profiles of velocity, as shown in Equation (43), confined to the fractional order $\alpha \in (0, 1]$, are shown by fixing the different times $t = 0.001$, $t = 0.1$, $t = 1$, and $t = 1{,}000$. As shown in Figures 6 and 7, it can be seen that for a short period of after $t = 0$, the velocity, as shown in Equation (43), under the condition of

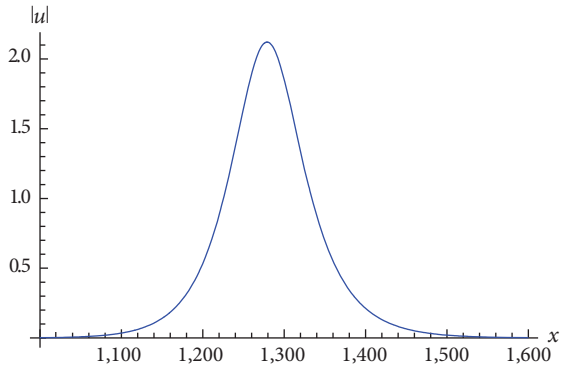

FIGURE 5: Fractional single solitons determined by Equation (42) with the fractional order $\alpha = 1/3$ at the time $t = 3{,}000$.

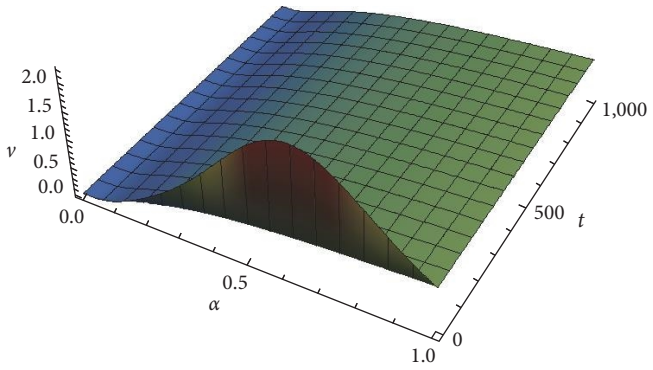

FIGURE 6: 3D image of velocity, as shown in Equation (43), confined to the fractional order $\alpha \in [0, 1]$ and time interval $t \in [0.001, 1{,}000]$.

$0 < \alpha < 1$, exhibits a significant rate of change, while at $\alpha = 1$, it always maintains $v \equiv 3/4$. For the specific fractional orders $\alpha = 1, \alpha = 7/9, \alpha = 3/5$, and $\alpha = 1/3$, we have:

$$v|_{\alpha=1} = \frac{3}{4},\ v|_{\alpha=7/9} = \frac{3^{9/7}}{4^{11/7}},\ v|_{\alpha=3/5} = \frac{3^{5/3}}{2^{10/3}},\ v|_{\alpha=1/3} = \frac{27}{64},\ (t \to +\infty), \tag{45}$$

and show the evolution trends of velocity, as shown in Equations (43) and (44), over time $t \in [0.001, 1{,}000]$ (Figure 8). As shown in Figure 8, the changes in the velocities gradually decrease until they stabilize. The initial velocities of fractional solitons are greater than that of the corresponding integer-order soliton, and then gradually becomes smaller than the case of integer-order soliton. Obviously, the smaller the fractional order α, the smaller the average speed calculated through Equations (43) and (44).

3.2. Fractional Semirational Solutions. Using the fractional single-soliton solution, as shown in Equations (41) and (42), and the second-step fractional GDT, as shown in Equations (32) and (33), we obtain the fractional semirational solutions of the fractional TCGH Equation (1):

$$u[2] = u[1] + 3i(\lambda_1 - \lambda_1^*)c_1 c_2^* \zeta, \tag{46}$$

$$v[2] = v[1] + 3i(\lambda_1 - \lambda_1^*)c_1 c_3^* \zeta, \tag{47}$$

where

$$\zeta = \frac{HG}{qHe^{\frac{3}{4}ip}\left(iD|c_1|^2 e^{\frac{3}{4}ip^*} + 4qe^{\frac{3}{4}ip}\right) + G|c_1|^2 e^{\frac{3}{4}ip^*}\left(4|c_1|^2 e^{-\frac{3}{4}ip} - iqFe^{-\frac{3}{4}ip^*}\right)}, \tag{48}$$

with

$$H = iA|c_1|^2 e^{-\frac{3}{4}ip} + 4qe^{-\frac{3}{4}ip^*},\ G = 4|c_1|^2 e^{\frac{3}{4}ip^*} - iqBe^{\frac{3}{4}ip}, \tag{49}$$

$$A = -4i + \frac{12\lambda_1}{\alpha}x^\alpha - \frac{12\lambda_1^*}{\alpha}(x^\alpha - 3\lambda_1 t^\alpha) + \frac{9(\lambda_1^*)^2(-4+3\lambda_1)}{\alpha}t^\alpha - \frac{27(\lambda_1^*)^3}{\alpha}t^\alpha, \tag{50}$$

$$B = 4i + \frac{12\lambda_1}{\alpha}x^\alpha + \frac{36\lambda_1^2}{\alpha}t^\alpha + \frac{27\lambda_1^3}{\alpha}t^\alpha - \frac{3\lambda_1^*}{\alpha}[4x^\alpha + 3\lambda_1(4+3\lambda_1)t^\alpha], \tag{51}$$

$$D = -4i + \frac{12\lambda_1}{\alpha}x^\alpha + \frac{36\lambda_1^2}{\alpha}t^\alpha + \frac{27\lambda_1^3}{\alpha}t^\alpha - \frac{3\lambda_1^*}{\alpha}[4x^\alpha + 3\lambda_1(4+3\lambda_1)t^\alpha], \tag{52}$$

$$F = 4i + \frac{12\lambda_1}{\alpha}x^\alpha - \frac{12\lambda_1^*}{\alpha}(x^\alpha - 3t^\alpha\lambda_1) + \frac{9(\lambda_1^*)^2(-4+3\lambda_1)}{\alpha}t^\alpha - \frac{27(\lambda_1^*)^3}{\alpha}t^\alpha, \tag{53}$$

$$p = \frac{\lambda_1}{\alpha}[4x^\alpha + 3t^\alpha\lambda_1(2+\lambda_1)],\ p^* = \frac{\lambda_1^*}{\alpha}[4x^\alpha + 3t^\alpha\lambda_1^*(2+\lambda_1^*)],\ q = |c_2|^2 + |c_3|^2. \tag{54}$$

Three special cases of the fractional semirational solutions, as shown in Equations (46) and (47), read:

Case 1. When $\lambda_1 = i, c_1 = 1, c_2 = 1$, and $c_3 = 1$,

$$u[2] = v[2] = -\frac{6e^{\frac{9(1+2i)}{4\alpha}t^\alpha + \frac{3}{\alpha}x^\alpha}\left[e^{\frac{6}{\alpha}x^\alpha}\left(4 + \frac{27+36i}{\alpha}t^\alpha - \frac{12}{\alpha}x^\alpha\right) + e^{\frac{9t^\alpha}{2\alpha}}\left(8 - \frac{54-72i}{\alpha}t^\alpha + \frac{24}{\alpha}x^\alpha\right)\right]}{8e^{\frac{9}{\alpha}t^\alpha} + 2e^{\frac{12}{\alpha}x^\alpha} + e^{\frac{9t^\alpha}{2\alpha}+\frac{6}{\alpha}x^\alpha}\left[8 + \frac{2025}{\alpha^2}(t^\alpha)^2 - \frac{648}{\alpha^2}t^\alpha x^\alpha + \frac{144}{\alpha^2}(x^\alpha)^2\right]}. \tag{55}$$

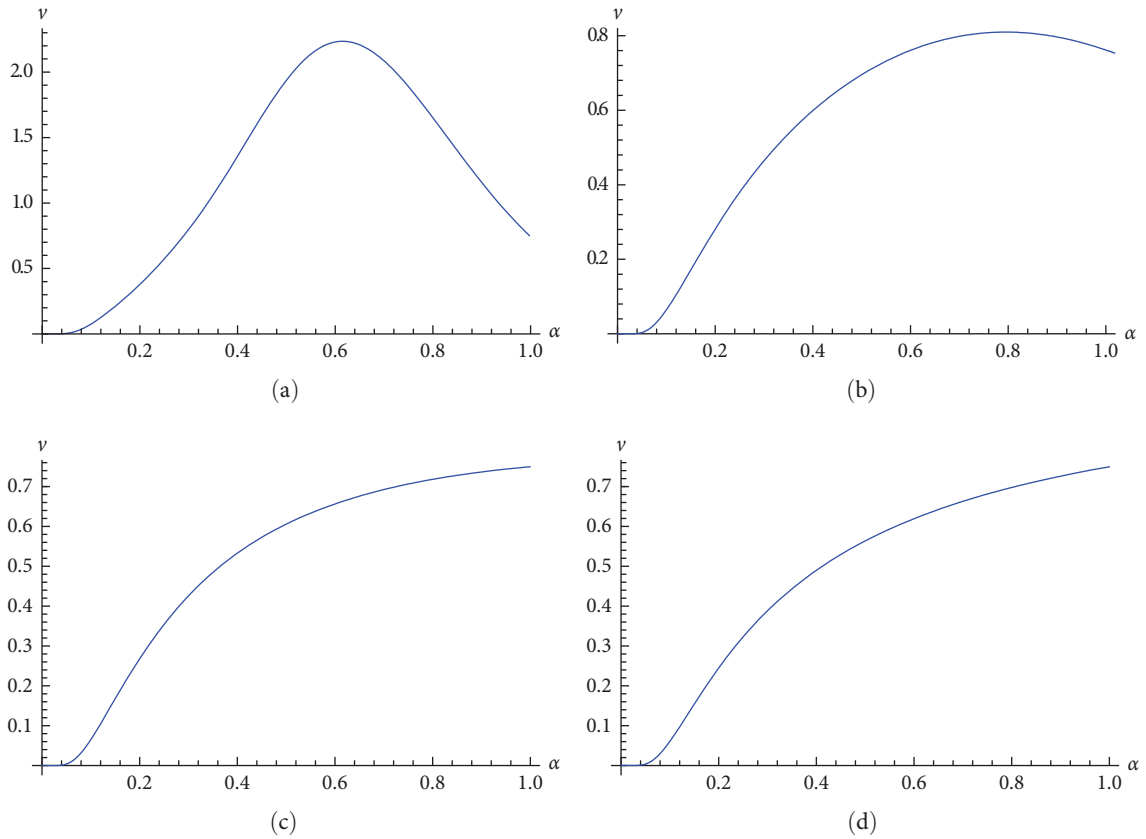

FIGURE 7: Profiles of velocity, as shown in Equation (43), confined to the fractional order $\alpha \in [0, 1]$ at the times: (a) $t = 0.001$, (b) $t = 0.1$, (c) $t = 1$, and (d) $t = 1{,}000$.

Case 2. When $\lambda_1 = -1 + i$, $c_1 = 2$, $c_2 = 1$, and $c_3 = 1$,

$$u[2] = v[2] = \frac{6e^{\frac{9(1-i)}{2\alpha}t^\alpha + \frac{3(1+i)}{\alpha}x^\alpha}\left[e^{\frac{9}{\alpha}t^\alpha}\left(-2 + \frac{18+9i}{\alpha}t^\alpha - \frac{6}{\alpha}x^\alpha\right) + 2e^{\frac{6}{\alpha}x^\alpha}\left(-2 - \frac{18-9i}{\alpha}t^\alpha + \frac{6}{\alpha}x^\alpha\right)\right]}{e^{\frac{18}{\alpha}t^\alpha} + 4e^{\frac{12}{\alpha}x^\alpha} + e^{\frac{9}{\alpha}t^\alpha + \frac{6}{\alpha}x^\alpha}\left[4 + \frac{810}{\alpha^2}(t^\alpha)^2 - \frac{432}{\alpha^2}t^\alpha x^\alpha + \frac{72}{\alpha^2}(x^\alpha)^2\right]}. \tag{56}$$

Case 3. When $\lambda_1 = -1 + i$, $c_1 = 1$, $c_2 = 2$, and $c_3 = 1$,

$$u[2] = v[2] = \frac{12e^{\frac{9(1-i)}{2\alpha}t^\alpha + \frac{3(1+i)}{\alpha}x^\alpha}\left[5e^{\frac{9}{\alpha}t^\alpha}\left(-2 + \frac{18+9i}{\alpha}t^\alpha - \frac{6}{\alpha}x^\alpha\right) + e^{\frac{6}{\alpha}x^\alpha}\left(-2 - \frac{18-9i}{\alpha}t^\alpha + \frac{6}{\alpha}x^\alpha\right)\right]}{25e^{\frac{18}{\alpha}t^\alpha} + e^{\frac{12}{\alpha}x^\alpha} + 5e^{\frac{9}{\alpha}t^\alpha + \frac{6}{\alpha}x^\alpha}\left[2 + \frac{405}{\alpha^2}(t^\alpha)^2 - \frac{216}{\alpha^2}t^\alpha x^\alpha + \frac{36}{\alpha^2}(x^\alpha)^2\right]}. \tag{57}$$

The 3D image of fractional semirational solution, as shown in Equation (55), is shown in Figures 9–12. As shown in Figure 9, the interactions between four right propagating double solitons with different fractional order values $\alpha = 1$, $\alpha = 7/9$, $\alpha = 3/5$, and $\alpha = 1/3$ generate second-order rogue waves. We call in this paper such a fractional soliton combined with fractional rogon as fractional solitrogon. As shown in Figures 10–12, the fractional double solitons and second-order solitrogons are shown at three different moments $t = -1$, $t = 0$, and $t = 1$. This indicates that the head-on collision that occurred, as shown in Figure 9, is elastic. Figures 10–12 also show that the fractional double solitons and second-order solitrogons are asymmetric. With the assistance of computer simulation, we found through comparison that the fractional double solitons and second-order solitrogons when $0 < \alpha < 1$ have a certain degree of tilt toward the vertical axis, with the tilt caused by the soliton on the right side, as shown in Figure 10(d), being more significant. In the interval $t \in [-1, 1]$, the wave widths of two-soliton change, with the solitons near vertical axis becoming narrower, while the other solitons become wider. The law of change is that the smaller the value of fractional order α, the

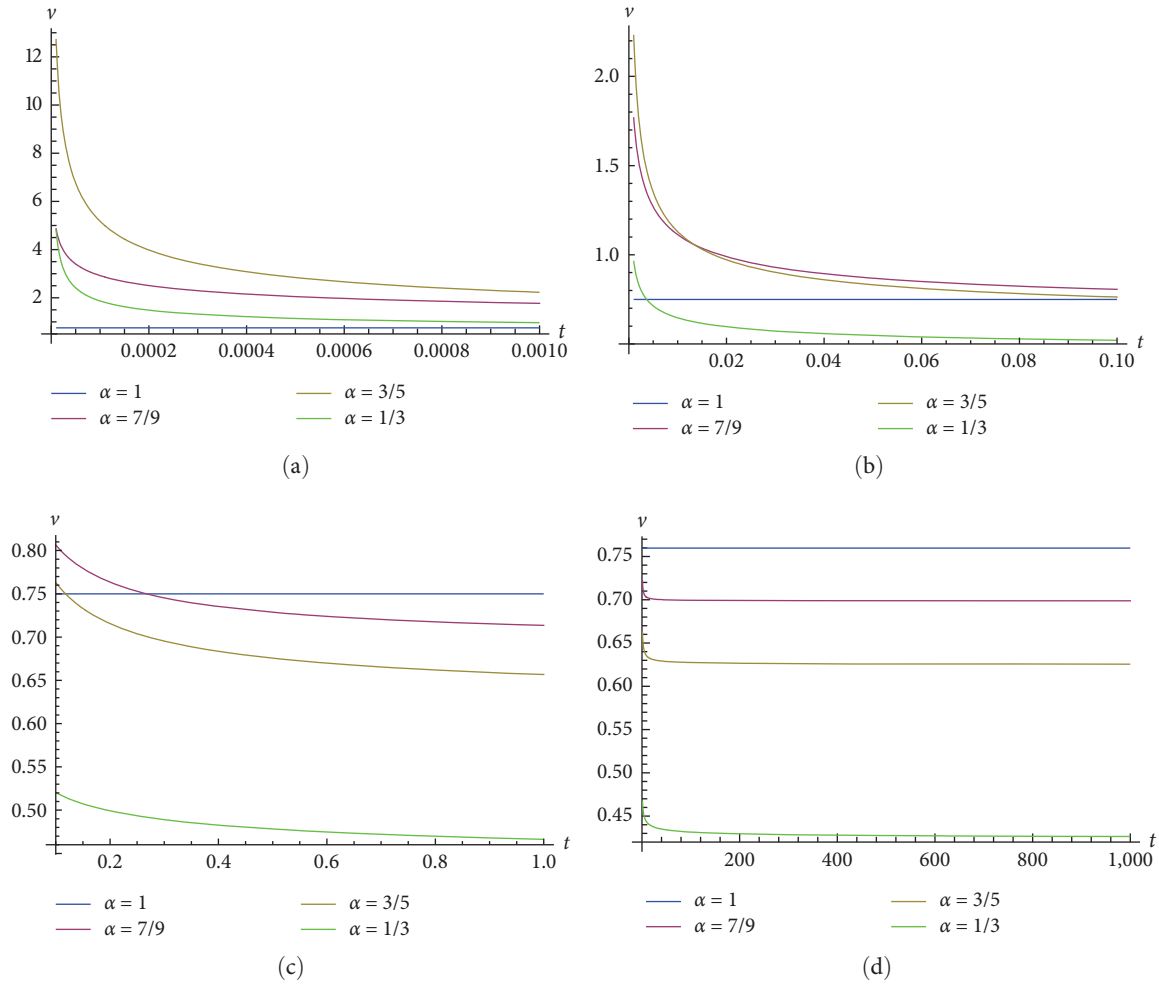

FIGURE 8: Evolution images of velocity, as shown in Equation (42), with different fractional orders $\alpha = 1$, $\alpha = 7/9$, $\alpha = 3/5$, and $\alpha = 1/3$ at the time intervals: (a) $t \in [0.00001, 0.001]$, (b) $t \in [0.01, 0.1]$, (c) $t \in [0.1, 1]$, and (d) $t \in [1, 1{,}000]$.

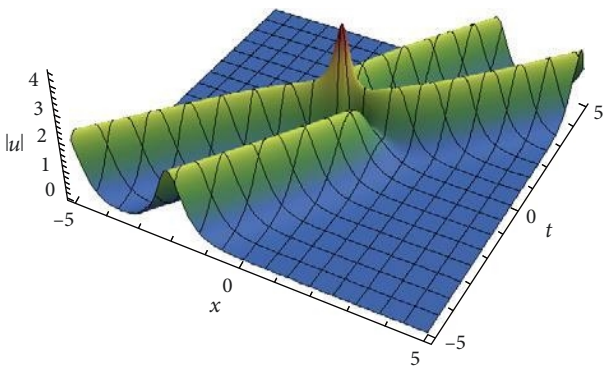

FIGURE 9: 3D image of fractional second-order solitrogon determined by Equation (55) with the fractional order $\alpha = 7/9$.

narrower/wider the wave widths near/far from the vertical axis, and the greater the tilt of wave crests toward the vertical axis.

Under the dominant effect of fractional order α, the velocities of double solitons and second-order solitrogons determined by Equation (55) are also time-varying. For a long period of time, the velocities have been decreasing, for example, if the time is limited to $t \in [0, 1{,}000]$, the smaller the fractional order α, the more significant the deceleration. Figure 13 shows that the smaller the fractional order α, and the shorter the end time of head-on collision interaction. At the beginning of the end of the interaction, as shown in Figure 14, we can see that the smaller the fractional order α, the slower the velocity of the soliton on the left, and the greater the velocity of the soliton on the right. At approximately $t = 50$, the propagation distances of the right solitons, as shown in Figure 15, are basically the same, while at $t = 70$, the propagation distances of the left and right solitons are all smaller than those of the integer-order soliton. As shown in Figures 13–16, as time increases, the tilt of the wave crests gradually weaken. When $t = 3{,}000$, the double soliton with the fractional $\alpha = 1/3$, as shown in Figure 16, almost no longer tilt.

4. Conclusion and Discussion

In summary, we would like to conclude that the proposed fractional TCGH Equation (1) is a fractional Lax integrable system. Owing to the fractional Lax pair, as shown in Equation (2), the fractional N-fold DT, as shown in Equations (21)–(23),

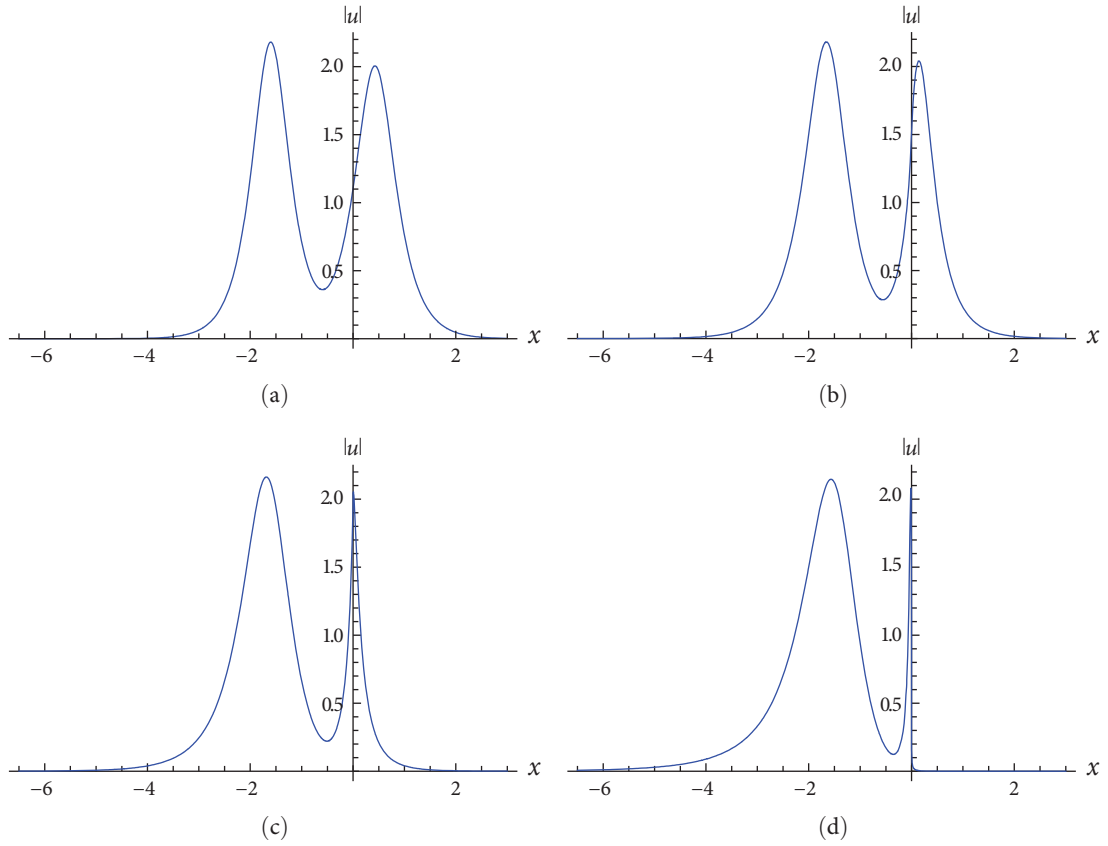

Figure 10: Fractional double solitons determined by Equation (55) with the different fractional orders: (a) $\alpha = 1$, (b) $\alpha = 7/9$, (c) $\alpha = 3/5$, and (d) $\alpha = 1/3$ at the time $t = -1$.

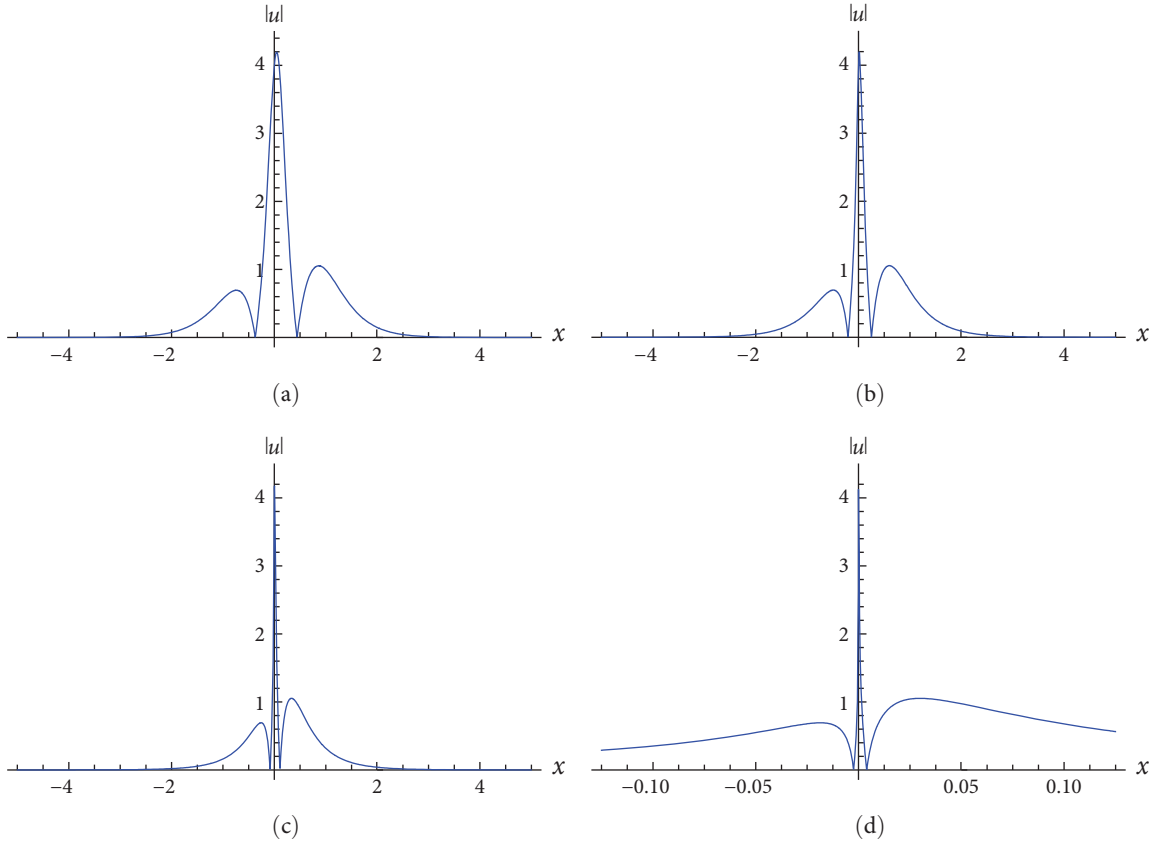

Figure 11: Fractional second-order solitrogons determined by Equation (55) with the different fractional orders: (a) $\alpha = 1$, (b) $\alpha = 7/9$, (c) $\alpha = 3/5$, and (d) $\alpha = 1/3$ at the time $t = 0$.

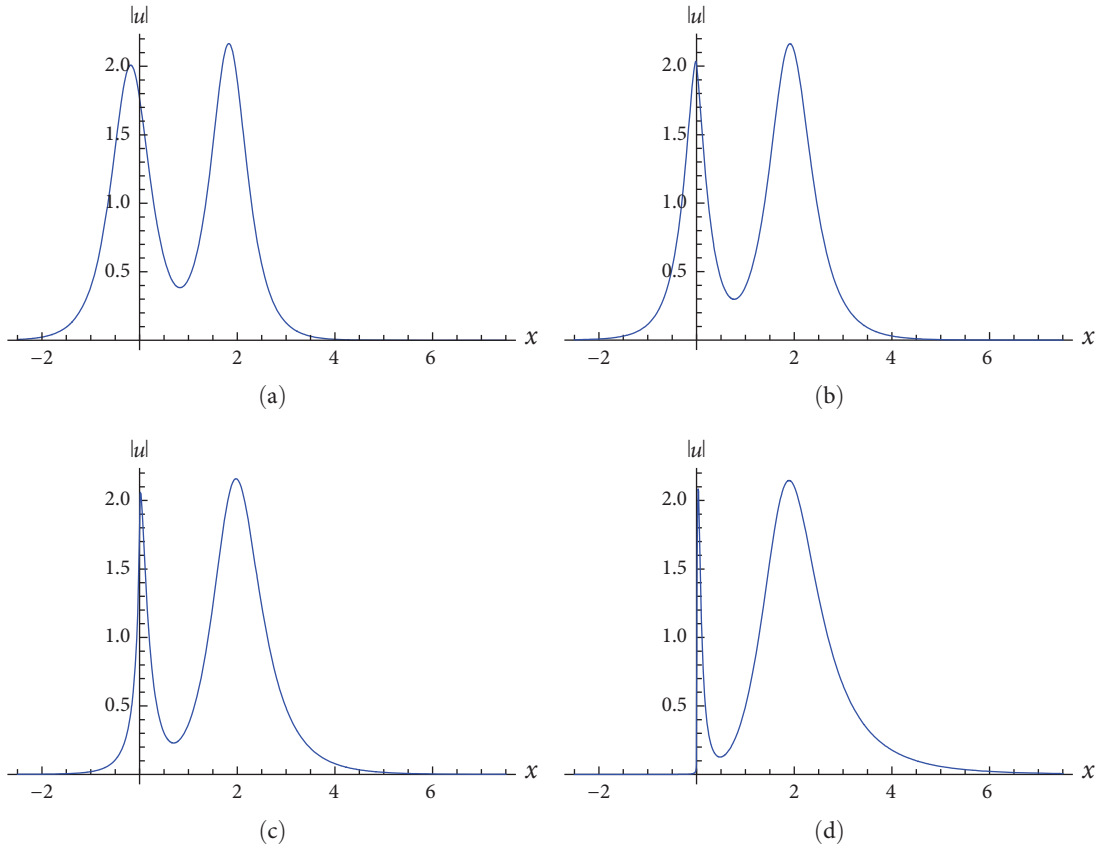

FIGURE 12: Fractional double solitons determined by Equation (55) with the different fractional orders: (a) $\alpha = 1$, (b) $\alpha = 7/9$, (c) $\alpha = 3/5$, and (d) $\alpha = 1/3$ at the time $t = 1$.

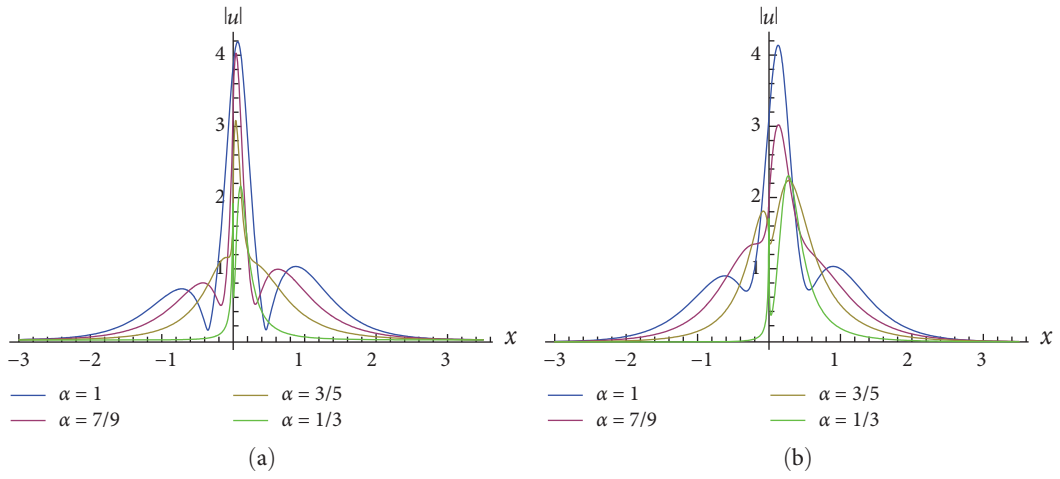

FIGURE 13: Continued.

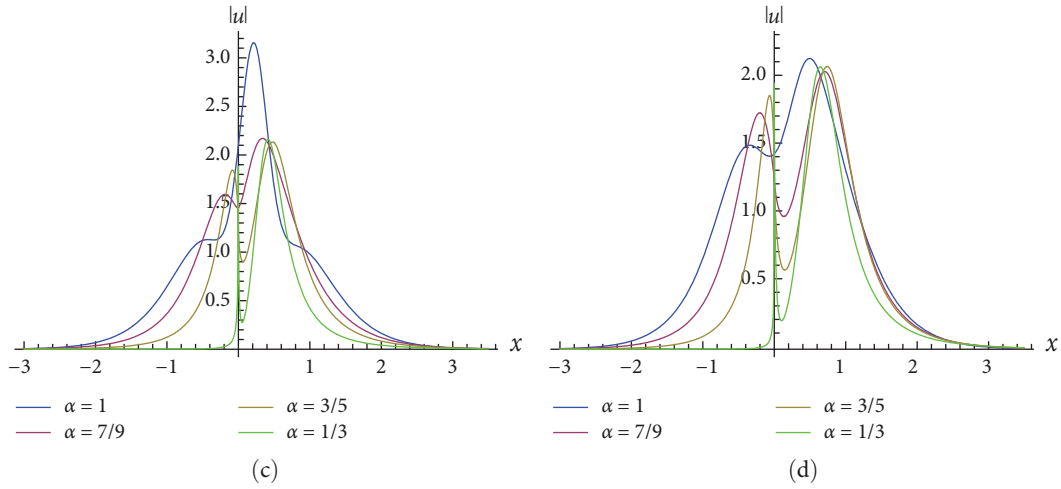

Figure 13: Fractional double solitons determined by Equation (55) with the different fractional orders $\alpha = 1$, $\alpha = 7/9$, $\alpha = 3/5$, and $\alpha = 1/3$ at the times: (a) $t = 0.01$, (b) $t = 0.05$, (c) $t = 0.07$, and (d) $t = 0.15$.

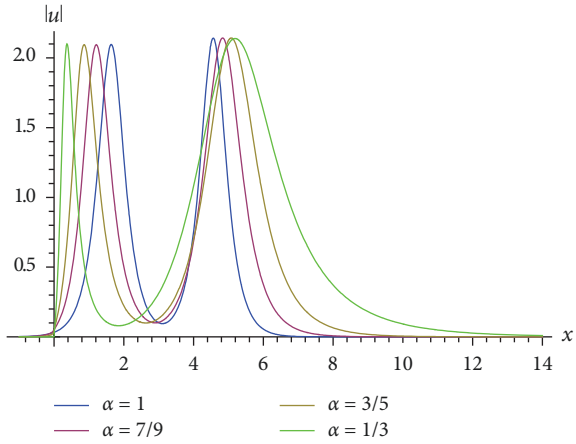

Figure 14: Fractional double solitons determined by Equation (55) with the different fractional orders $\alpha = 1$, $\alpha = 7/9$, $\alpha = 3/5$, and $\alpha = 1/3$ at the time $t = 4$.

was derived. Based on the derived fractional N-fold DT, as shown in Equations (21)–(23), the first-step fractional GDTs, as shown in Equations (26)–(28), second-step fractional GDTs, as shown in Equations (31)–(33), and third-step fractional GDTs, as shown in Equations (36)–(38), of the fractional TCGH Equation (1) were constructed, respectively. Then, the fractional soliton solutions, as shown in Equations (40) and (41), and semirational solutions, as shown in Equations (46) and (47), were obtained by using Equations (27), (28), (32), and (33). This indicates that one advantage of the fractional DT and GDT presented in this article is that they can be used to handle fractional integrable systems.

Because the fractional TCGH Equation (1) is a high-order integrable system, its integrability requires that the degree of the matrix polynomial M of spectral parameter λ in the x-part of fractional Lax pair, as shown in Equations (2) and (3), remains unchanged, that is, U_0 and U_1 are fixed, then the matrix N in the t-part of fractional Lax pair, as shown in Equations (2) and (3), must be a cubic polynomial of λ with the coefficients V_0, V_1, V_2, and V_3. Based on the fractional Lax pair, as shown in Equations (2) and (3), in this case, we obtained the fractional N-soliton solutions, as shown in Equations (22) and (23), for arbitrary integer $N \geq 1$, but did not specifically discuss higher-order soliton solutions, nor we obtain semirational solutions of third order or higher. On one hand, it is because this article focused on studying the feasibility of obtaining semirational solutions through examples, and on the other hand, it is not only the complexity of higher-order semirational solutions but also the similarity of their dynamic properties.

As it is well known, the results obtained by numerical algorithms are usually approximations of real solutions that satisfy a certain degree of accuracy. However, it is generally difficult or even impossible for numerical algorithms to obtain either exact solutions with complex representations or high-precision approximate solutions under complex initial conditions, such as the semirational solutions, as shown in Equation (46), or fractional N-soliton solutions, as shown in Equations (22) and (23). This is a significant advantage of the fractional DT and GDT over numerical methods.

It is shown that compared to integer-order solitons and solitrogons, the fractional ones obtained in this paper have significant characteristics. One is that fractional solitons and solitrogons tilt to a certain extent, gradually decelerate and widen until their velocities and wave widths stabilize and the tilt gradually disappears, and the other is the similar asymmetry [34] of fractional solitons and solitrogons. The deceleration propagation of fractional solitons and solitrogons is consistent with the anomalous diffusion phenomenon that occurs in the background of fractional dimensions. These are novel for fractional integrable systems, which indicate the propagation laws of decelerating solitons and solitrogons in fractional dimensional media, and also provide useful references for the regulatory mechanism dominated by fractional order to form highly asymmetric rogue waves.

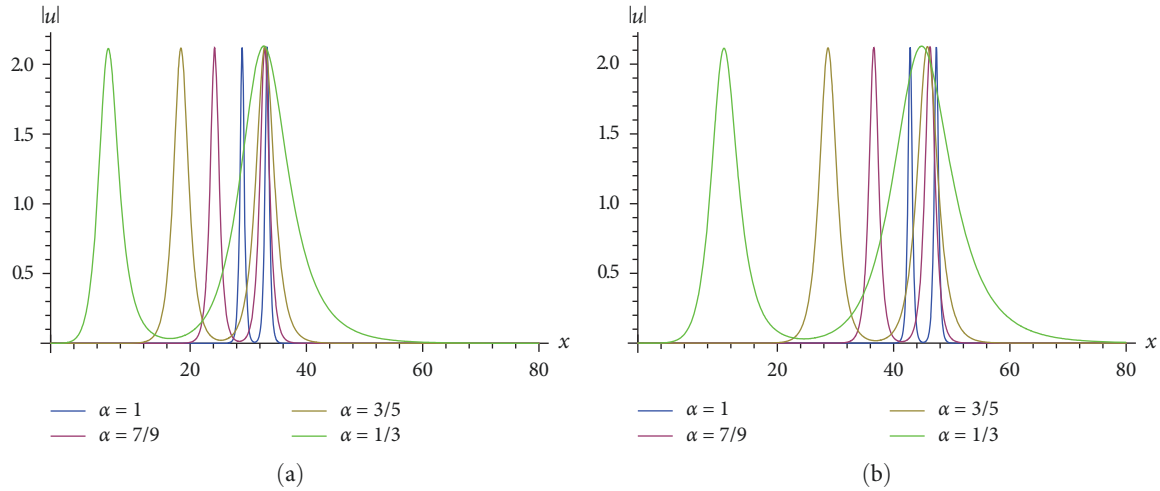

FIGURE 15: Fractional double solitons determined by Equation (55) with the different fractional orders $\alpha = 1$, $\alpha = 7/9$, $\alpha = 3/5$, and $\alpha = 1/3$ at the times: (a) $t = 50$ and (b) $t = 70$.

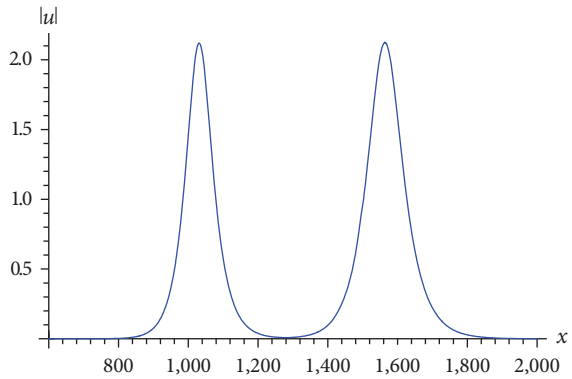

FIGURE 16: Fractional double solitons determined by Equation (55) with the fractional order $\alpha = 1/3$ at the time $t = 3{,}000$.

Data Availability

All data supporting the findings of this study are available within the article.

Conflicts of Interest

The authors declare that there is no conflicts of interest regarding the publication of this article.

Acknowledgments

This work was supported by the Liaoning BaiQianWan Talents Program of China (2020921037), the National Science Foundation of China (11547005), and the Natural Science Foundation of Education Department of Liaoning Province of China (LJ2020002).

References

[1] I. Podlubny, *Fractional Differential Equations: An Introduction to Fractional Derivatives, Fractional Differential Equations, to Methods of Their Solution and Some of Their Applications*, vol. 198 of Mathematics in Science and Engineering, Academic Press, New York, Article ID 366, 1998.

[2] B. Xu, Y. Zhang, and S. Zhang, "Analytical methods for nonlinear fractional Kolmogorov–Petrovskii–Piskunov equation: Soliton solution and operator solution," *Thermal Science*, vol. 25, no. 3B, pp. 2161–2168, 2021.

[3] N. Laskin, "Fractional quantum mechanics," *Physical Review E*, vol. 62, no. 3, pp. 3135–3145, 2000.

[4] S. Zhang, Y. Y. Wei, and B. Xu, "Fractional soliton dynamics and spectral transform of time-fractional nonlinear systems: a concrete example," *Complexity*, vol. 2019, Article ID 7952871, 9 pages, 2019.

[5] B. Xu, Y. Zhang, and S. Zhang, "Fractional isospectral and non-isospectral AKNS hierarchies and their analytic methods for *N*-fractal solutions with Mittag-Leffler functions," *Advances in Difference Equations*, vol. 2021, Article ID 223, 2021.

[6] B. Xu, Y. Zhang, and S. Zhang, "Line soliton interactions for shallow ocean-waves and novel solutions with peakon, ring, conical, columnar and lump structures based on fractional KP equation," *Advances in Mathematical Physics*, vol. 2021, Article ID 6664039, 15 pages, 2021.

[7] M. J. Ablowitz, J. B. Been, and L. D. Carr, "Fractional integrable nonlinear soliton equation," *Physical Review Letters*, vol. 128, no. 18, Article ID 184101, 2022.

[8] M. J. Ablowitz, J. B. Been, and L. D. Carr, "Integrable fractional modified Korteweg-deVries, sine-gordon, and sinh-gordon equations," *Journal of Physics A: Mathematical and Theoretical*, vol. 55, no. 38, Article ID 384010, 2022.

[9] M. J. Ablowitz, J. B. Been, and L. D. Carr, "Fractional integrable and related discrete nonlinear Schrödinger equations," *Physics Letters A*, vol. 452, Article ID 128459, 2022.

[10] Z. Yan, "New integrable multi-Lévy-index and mixed fractional nonlinear soliton hierarchies," *Chaos Solitons & Fractals*, vol. 164, Article ID 112758, 2022.

[11] W. Weng, M. Zhang, G. Zhang, and Z. Yan, "Dynamics of fractional *N*-soliton solutions with anomalous dispersions of integrable fractional higher-order nonlinear Schrödinger equations," *Chaos*, vol. 32, no. 12, Article ID 123110, 2022.

[12] M. J. Ablowitz and D. E. Baldwin, "Nonlinear shallow oceanwave soliton interactions on flat beaches," *Physical Review E*, vol. 86, no. 3, Article ID 036305, 2012.

[13] M. J. Ablowitz and P. A. Clarkson, *Solitons, Nonlinear Evolution Equations and Inverse Scattering*, Cambridge University Press, 1991.
[14] R. Hirota, "Exact envelope-soliton solutions of a nonlinear wave equation," *Journal of Mathematical Physics*, vol. 14, no. 7, pp. 805–809, 1973.
[15] R. S. Tasgal and M. J. Potasek, "Soliton solutions to coupled higher-order nonlinear Schrödinger equations," *Journal of Mathematical Physics*, vol. 33, no. 3, pp. 1208–1215, 1992.
[16] K. Porsezian and K. Nakkeeran, "Optical solitons in birefringent fibre—Bäcklund transformation approach," *Pure and Applied Optics: Journal of the European Optical Society Part A*, vol. 6, no. 1, Article ID L7, 1997.
[17] S. Chen and L.-Y. Song, "Rogue waves in coupled Hirota systems," *Physical Review E*, vol. 87, no. 3, Article ID 032910, 2013.
[18] A. Ankiewicz, J. M. Soto-Crespo, and N. Akhmediev, "Rogue waves and rational solutions of the Hirota equation," *Physical Review E*, vol. 81, no. 4, Article ID 046602, 2010.
[19] R. Guo, H.-H. Zhao, and Y. Wang, "A higher-order coupled nonlinear Schrödinger system: solitons, breathers, and rogue wave solutions," *Nonlinear Dynamics*, vol. 83, pp. 2475–2484, 2016.
[20] R. Khalil, M. Al Horani, A. Yousef, and M. Sababheh, "A new definition of fractional derivative," *Journal of Computational and Applied Mathematics*, vol. 264, pp. 65–70, 2014.
[21] X.-Y. Xie and X.-B. Liu, "Elastic and inelastic collisions of the semi-rational solutions for the coupled Hirota equations in a birefringent fiber," *Applied Mathematics Letters*, vol. 105, Article ID 106291, 2020.
[22] C. S. Gardner, J. M. Greene, M. D. Kruskal, and R. M. Miura, "Method for solving the Korteweg—deVries equation," *Physical Review Letters*, vol. 19, no. 19, pp. 1095–1097, 1967.
[23] R. Hirota, "Exact solution of the Korteweg—deVries equation for multiple collisions of solitons," *Physical Review Letters*, vol. 27, no. 18, pp. 1192–1194, 1971.
[24] M. Wang, "Exact solutions for a compound KdV-burgers equation," *Physics Letters A*, vol. 213, no. 5-6, pp. 279–287, 1996.
[25] J.-H. He and X.-H. Wu, "Exp-function method for nonlinear wave equations," *Chaos Solitons & Fractals*, vol. 30, no. 3, pp. 700–708, 2006.
[26] A. M. A. El-Sayed, S. Z. Rida, and A. A. M. Arafa, "Exact solutions of fractional-order biological population model," *Communications in Theoretial Physics*, vol. 52, no. 6, Article ID 992, 2009.
[27] S. Deng and X. Ge, "The variational iteration method for Whitham–Broer–Kaup system with local fractional derivatives," *Thermal Science*, vol. 26, no. 3 Part B, pp. 2419–2426, 2022.
[28] X.-J. Yang, H.-M. Srivastava, and C. Cattani, "Local fractional homotopy perturbation method for solving fractal partial differential equations arising in mathematical physics," *Romanian Reports in Physics*, vol. 67, no. 3, pp. 752–761, 2015.
[29] V. B. Matveev and M. Salle, *Darboux Transformation and Soliton*, Springer, Berlin, 1991.
[30] B. L. Guo, L. X. Tian, Z. Y. Yan, and L. M. Ling, *Rogue Wave and Its Mathematical Theory*, Zhejiang Science and Technology Press, Zhejiang, 2015.
[31] B. Guo, L. Ling, and Q. P. Liu, "Nonlinear Schrödinger equation: generalized darboux transformation and rogue wave solutions," *Physical Review E*, vol. 85, no. 2, Article ID 026607, 2012.
[32] Y. Jiang and Q.-X. Qu, "Some semirational solutions and their interactions on the zero-intensity background for the coupled nonlinear Schrödinger equations," *Communications in Nonlinear Science and Numerical Simulation*, vol. 67, pp. 403–413, 2019.
[33] B. Xu, P. Shi, and S. Zhang, "Non-differntiable fractional odd-soliton solutions of local fractional generalized Broer–Kaup system by extending Darboux transformation," *Thermal Science*, vol. 27, no. Spec. Issue 1, pp. 77–86, 2023.
[34] S. Zhang, F. Zhu, and B. Xu, "Localized symmetric and asymmetric solitary wave solutions of fractional coupled nonlinear Schrödinger equations," *Symmetry*, vol. 15, no. 6, Article ID 1211, 2023.